

1 **Experimentally Evolved *Staphylococcus aureus* Survives in the Presence of *Pseudomonas***
2 ***aeruginosa* by Acquiring Mutations in the Amino Acid Transporter, GltT**

3 Ashley M. Alexander ^{a,c,d}, Justin M. Luu ^{b,d}, Vishnu Raghuram ^{b,c,d}, Giulia Bottacin ^e, Simon van Vliet ^{e,f},
4 Timothy D. Read ^c, Joanna B. Goldberg ^d

5
6 ^a Population Biology, Ecology, and Evolution Program, Graduate Division of Biological and Biomedical
7 Sciences, Laney Graduate School, Emory University, Atlanta, Georgia, USA

8
9 ^b Microbiology and Molecular Genetics Program, Graduate Division of Biological and Biomedical
10 Sciences, Laney Graduate School, Emory University, Atlanta, Georgia, USA

11
12 ^c Division of Infectious Diseases and Department of Human Genetics, Emory University School of
13 Medicine, Atlanta, Georgia, USA

14
15 ^d Department of Pediatrics, Division of Pulmonology, Asthma, Cystic Fibrosis, and Sleep, Emory
16 University School of Medicine, Atlanta, Georgia, USA

17
18 ^e Biozentrum, University of Basel, Spitalstrasse 41, 4056 Basel, Switzerland

19
20 ^f Department of Fundamental Microbiology, University of Lausanne, Quartier Unil-Sorge, 1015
21 Lausanne, Switzerland

22

23 Keywords: *Staphylococcus aureus*, *Pseudomonas aeruginosa*, cystic fibrosis, interspecies
24 competition, Experimental Evolution, amino acid metabolism

25

26 Running Title: *S. aureus gltT* mutants survive with *P. aeruginosa* (48/54 characters)

27

28 **Abstract (232/250 words)**

29 *Staphylococcus aureus* and *Pseudomonas aeruginosa* are the most common bacterial pathogens
30 isolated from cystic fibrosis (CF) related lung infections. When both of these opportunistic pathogens
31 are found in a coinfection, CF patients tend to have higher rates of pulmonary exacerbations and
32 experience a more rapid decrease in lung function. When cultured together under standard laboratory
33 conditions, it is often observed that *P. aeruginosa* effectively inhibits *S. aureus* growth. Previous work
34 from our group revealed that *S. aureus* from CF infections have isolate-specific survival capabilities
35 when cocultured with *P. aeruginosa*. In this study, we designed a serial transfer evolution experiment to
36 identify mutations that allow *S. aureus* to adapt to the presence of *P. aeruginosa*. Using *S. aureus*
37 USA300 JE2 as our ancestral strain, populations of *S. aureus* were repeatedly cocultured with fresh *P.*
38 *aeruginosa* strain, PAO1. After 8 coculture periods, *S. aureus* populations that survived better in the
39 presence of PAO1 were observed. We found two independent mutations in the highly conserved *S.*
40 *aureus* aspartate transporter, *gltT*, that were unique to evolved *P. aeruginosa*-tolerant isolates.
41 Subsequent phenotypic testing demonstrated that *gltT* mutants have reduced uptake of glutamate and
42 outcompete wild-type *S. aureus* when glutamate is absent from chemically-defined media. These
43 findings together demonstrate that the presence of *P. aeruginosa* exerts selective pressure on *S.*
44 *aureus* to alter its uptake and metabolism of key amino acids when the two bacteria are cultured
45 together.

46

47 **Importance (144/150 words)**

48 *Staphylococcus aureus* and *Pseudomonas aeruginosa* are the two most common bacterial pathogens
49 that infect people with the genetic disease, cystic fibrosis (CF). They are often found together in CF-
50 associated polymicrobial infections that are associated with worse patient prognosis. Understanding
51 how these very different opportunistic pathogens influence each other in a shared environment is
52 pertinent to improving the treatment of polymicrobial infections. While much attention has been brought
53 to the interspecific interactions between *S. aureus* and *P. aeruginosa*, few studies have used
54 experimental evolution methods to identify determinants of their competition and coexistence. Here, we
55 use a serial transfer experimental evolution approach and identified a single genetic change associated
56 with improved survival of *S. aureus* in the presence of *P. aeruginosa*. Our findings implicate metabolism
57 of shared resources as an important factor in *S. aureus*'s ability to survive in the presence of *P.*
58 *aeruginosa*.

59

60 **Introduction**

61 Often, a community of microbes contributes to the shaping of the infection environment through
62 metabolic interactions, altering adaptive trajectories, or changing the antibiotic susceptibilities of
63 interacting strains (Brown et al., 2008, 2012; Dalton et al., 2011; Stacy et al., 2016; Wadsworth et al.,
64 2018). In the case of chronic infections, multiple opportunistic pathogens can coexist in their shared
65 host environment for many generations, exerting their own respective selective pressures on each
66 other (Hamelin et al., 2019). Pairwise interactions between coexisting opportunistic pathogens such as
67 *Staphylococcus aureus* and *Pseudomonas aeruginosa* have become a topic of great interest to
68 microbiologists both for the importance of the interaction to the course of the genetic disease cystic
69 fibrosis (CF) and as model system for pathogen coevolution (Barraza & Whiteley, 2021; Camus et al.,
70 2020).

71

72 In 2021, 32,100 people were documented as living with CF in the United States, a genetic disease that
73 impacts multiple organ systems and greatly reduces life-expectancy and requires lifelong treatment
74 (Cystic Fibrosis Foundation, 2021). One of the major complications of this disease is an increased risk
75 for developing chronic respiratory infections that are exacerbated by the buildup of respiratory sputum.
76 Over the last decade, *S. aureus* has displaced *P. aeruginosa* as the most common infective agent
77 responsible for respiratory infections in people with CF and is detected in as many as 70% of CF
78 associated lung infections. *S. aureus* is the predominant pathogen infecting young people with CF;
79 older patients are more likely to be infected with *P. aeruginosa* and many individuals maintain both
80 pathogens in coinfections (Cystic Fibrosis Foundation, 2021). Coinfections with *P. aeruginosa* and *S.*
81 *aureus* may persist in the same patient for many years and even decades (Bernardy et al., 2020;
82 Camus et al., 2020; Fischer et al., 2020). Chart reviews of more than 200 patients have revealed that
83 coinfecting patients experience significantly more pulmonary exacerbations and a more rapid decline in
84 lung function compared to those with monoinfections of *S. aureus* or *P. aeruginosa* (Limoli et al., 2016).
85

86 When *P. aeruginosa* and *S. aureus* are cultured together outside of a host, there are a range of
87 outcomes that may be dependent on strain identity or environmental conditions (Bernardy et al., 2022;
88 Filkins et al., 2015; Limoli et al., 2017; Mashburn et al., 2005). Previously, our group observed that *S.*
89 *aureus* isolated from CF patients range from highly sensitive to tolerant in their ability to coexist with the
90 lab-adapted strain of *P. aeruginosa*, PAO1. Sensitive clinical isolates experienced as much as a 6-fold
91 decrease in recovered colony-forming units (CFUs) after coculture, while others maintained most of
92 their population, experiencing less than a 2-fold decrease in population size (Bernardy et al., 2020).
93 We have also observed that *S. aureus* is able to adapt to the presence of *P. aeruginosa* in its
94 environment by showing that co-isolated *S. aureus* and *P. aeruginosa* strains grow better compared to
95 non-concurrent isolates (Bernardy et al., 2022). Additionally, other groups have found that fermentative
96 metabolism, polysaccharide production, and toxin excretion are all important phenotypes for *S. aureus*

97 in its coexistence with *P. aeruginosa* (Filkins et al., 2015; Wieneke et al., 2021). It is also known that *S.*
98 *aureus* can adapt to *P. aeruginosa* bactericidal compounds such as 2-heptyl-4-hydroxyquinoline-N-
99 oxide (HQNO) and pyocyanin and that such adaptations may impact antibiotic resistance profiles of
100 either species (Filkins et al., 2015; Limoli et al., 2016; Nguyen et al., 2014; Orazi & O'Toole, 2017).

101

102 In this study we sought to gain a greater understanding for how *S. aureus* adapts to the presence of *P.*
103 *aeruginosa* and which *S. aureus* genotypes/phenotypes are under strong selective pressure in their
104 shared environment. We showed that *S. aureus* adapted to the negative selective pressures presented
105 by *P. aeruginosa* in a serial transfer evolution experiment. We found that rather than adapting to
106 secreted toxins or contact dependent killing, *S. aureus* reduced its uptake of aspartate by disrupting its
107 singular aspartate transporter, *gltT* (Potter et al., 2020). We hypothesize that loss of function of this
108 membrane transporter results in *S. aureus* becoming more resilient to fluctuations in nutrient availability
109 caused by the presence of *P. aeruginosa* in its environment. These results are surprising given that *P.*
110 *aeruginosa* has other well-characterized mechanisms for directly inhibiting *S. aureus* in its environment,
111 however, our findings suggest that optimizing amino acid metabolism is a potential pathway for
112 adaptation for *S. aureus* that co-occurs with *P. aeruginosa*.

113

114 **Methods**

115 Bacterial Strains

116 *Staphylococcus aureus* USA 300 strain JE2 (Kennedy et al., 2008, 2010) was used as the ancestral
117 strain for experimental evolution with *Pseudomonas aeruginosa* strain PAO1. Using the Nebraska
118 Transposon Mutant Library (NTML) (Fey et al., 2013) an isogenic JE2 *gltT* mutant (*SAUSA300_2329*)
119 was obtained and transduced into our own JE2 background. To do this we amplified the *gltT* locus with
120 the transposon from *SAUSA300_2329*. The *gltT* gene with the inserted transposon was then confirmed

121 and amplified by PCR and then transduced into our parental JE2 strain using phage ϕ 11 (landolo et al.,
122 2002) to generate strain JE2 *gltT*::Tn, as described below.

123

124 In brief, transduction was carried out by first preparing fresh ϕ 11 lysate first with *S. aureus* strain
125 RN4220. Collected lysate was then inoculated with NTML isolate SAUSA300_2329 and titers were
126 measured at 3×10^8 pfu/mL. Transduction was then carried out with a multiplicity of infection of 0.1
127 according to methods in Krausz & Bose (2016). Transduced colonies were isolated on Trypticase Soy
128 Agar (TSA) plates with 25 μ g/mL erythromycin and confirmed by PCR, identifying the presence of the
129 complete transposon at the correct site on the chromosome. Primer sequences used to confirm
130 transposon by amplicon size – 5' AAAATTAGCCTACCTATGCAAGTTGT 3' and 5'
131 TTTTGCTTTGTCATATACGTTTTCC 3'. We also used transposon specific primers to amplify from
132 within the transposon and the gene itself using primers (negative strand) 5'
133 GCTTTTTCTAAATGTTTTTAAAGTAAATCAAGTAC 3' and (positive strand) 5'
134 CTCGATTCTATTAACAAGGG 3', as described by Fey et al. (2013).

135

136 Fluorescently labeled strains were generated by transforming multicopy plasmids obtained from Dr.
137 Marvin Whiteley's lab (Georgia Institute of Technology), pCM29 (Pang et al., 2010) and pHC48
138 (Ibberson et al., 2016) into both JE2 and JE2 *gltT*::Tn via electroporation (Grosser & Richardson, 2016).
139 This gave us the fluorescently labeled set of JE2.GFP, JE2.DsRed and JE2 *gltT*::Tn.GFP and JE2
140 *gltT*::Tn.DsRed (**Table 1**).

141

142 Media

143 Cocultures for evolution experiments and phenotyping were conducted on TSA. After each coculture
144 period each species was isolated on their respective isolation agar, Pseudomonas Isolation agar (PIA;
145 BD Difco) and Staphylococcus isolation agar (SIA; BD Difco TSA with 7.5% NaCl). For liquid cultures,
146 bacteria were cultured in lysogeny broth (LB; Teknova) which was supplemented with erythromycin (25

147 $\mu\text{g/mL}$) to select for transposon mutants and/or chloramphenicol (10 $\mu\text{g/mL}$) to maintain fluorescent
148 plasmids. Chemically defined media with glucose (CDMG) was made according to Hussain et al.
149 (1991), with varying levels of aspartate (1.1 mM or 2.2 mM) and glutamate (1.0 mM or 2.0 mM), as
150 needed. CDMG batches were always used within 5 days and stored at room temperature, in the dark.
151 Depleted Trypticase Soy Broth (TSB) medium, used for single-cell microscopy, was prepared by
152 diluting an overnight culture of PAO1 1:100 into 10 mL TSB and growing the culture for either 3 or 16
153 hours before filter sterilizing (0.2 μm filter, Sarstedt) to remove cells from the supernatant.

154

155 Experimental evolution

156 Before being cultured with *P. aeruginosa* PAO1, 4 single colony isolates of JE2 were picked and grown
157 overnight in 3 mL of LB media in a test tube at 37°C in a rolling incubator. 10 μL of an overnight culture
158 was then inoculated on 0.45 μm filters (MF-Millipore® Membrane Filter) on TSA and cultured at 37°C
159 for 24 hours. Each filter was collected, and adhering cells were resuspended in 1.5 mL of LB media by
160 vortexing for 30 seconds. To prepare *P. aeruginosa* for coculturing, a single colony of PAO1 was
161 incubated in 3 mL of LB media overnight at 37°C in a rolling incubator. The optical density 600nm
162 (OD_{600}) of the resuspended *S. aureus* as well as the overnight PAO1 culture was measured. Cultures
163 were normalized to the same OD by diluting the PAO1 overnight culture in LB before inoculating a
164 coculture at a ratio of 30:1 (*S. aureus*:*P. aeruginosa*). A 30:1 inoculum ratio was determined through
165 preliminary experiments to exert optimal amount selective pressure on *S. aureus* at without risking a
166 population level extinction (approximately a 4-fold decrease in population size after coculture). 10 μL of
167 coculture mixture was inoculated onto 0.45 μm filters on TSA plates and incubated at 37°C for 48
168 hours. To account for any adaptation to culture conditions, control populations of JE2 were passaged
169 alongside experimental populations under identical conditions, but never cocultured with *P. aeruginosa*.
170
171 Each subsequent coculture was carried out by recovering filters and vortexing them in 1.5 mL of LB
172 media for 30 seconds to collect adhering cells. Resuspended cell mixtures were serially diluted and

173 plated for CFUs on SIA and PIA. 50 μ l of resuspended coculture was also plated on SIA to be used to
174 inoculate the next coculture (**Figure 1A**). After at least 24 hours of incubation at 37°C, isolated *S.*
175 *aureus* was then collected off SIA plates with an inoculation loop and resuspended in LB media. This
176 suspension was used to inoculate the next coculture period as well as to create a glycerol stock of the
177 recovered population of *S. aureus*. PAO1 liquid cultures were incubated overnight at 37°C and then
178 measured at OD₆₀₀ and diluted to the same OD₆₀₀ of the resuspended culture of *S. aureus* before being
179 mixed at a ratio of 30:1. Inoculum densities fluctuated throughout the experiment based on the amount
180 of *S. aureus* that could be recovered from the previous coculture period. Total inoculum densities
181 ranged between 10⁸-10¹⁰ CFUs. We designed the experiment with an initial large population of *S.*
182 *aureus* (10⁸-10¹⁰ CFUs) to mimic the event of *P. aeruginosa* invading an established *S. aureus*
183 population as is often the case in CF-associated respiratory infections (Cystic Fibrosis Foundation,
184 2021).

185

186 Whole genome sequencing

187 Single colonies were isolated from evolved *S. aureus* populations and control populations and were
188 used to inoculate overnight cultures and subsequent glycerol freezer stocks. Isolates were later struck
189 out on SIA plates and incubated overnight at 37°C. Cells were collected off plates with an inoculation
190 loop the next day and resuspended in 480 μ l of EDTA. *S. aureus* cells were then lysed by adding 20 μ l
191 of 10 mg/mL lysozyme and 20 μ l of 5 mg/mL lysostaphin to the resuspended cell mixture. This mixture
192 was then incubated at 37°C for one hour before proceeding with the rest of the protocol outlined for the
193 Promega Wizard genomic DNA purification kit (Silberstein et al., 2018). Genomic DNA was sequenced
194 using the Illumina NextSeq 2000 platform at the Microbial Genome Sequencing Center (Pittsburgh,
195 PA). Whole genome sequences were evaluated for quality using the program FASTQC (Wingett &
196 Andrews, 2018) and adapter sequences were removed using Trimmomatic (Bolger et al., 2014).

197 Sequences were then screened for variants using Snippy with JE2 NCBI NC_007793.1 sequence as a
198 reference (Seeman, 2015).

199

200 Complementation of *gltT*

201 The *gltT* gene was cloned using the multicopy pOS1 shuttle vector with the constitutive plgT promoter
202 (Bubeck Wardenburg et al., 2006; Schneewind et al., 1992). The ancestral gene was amplified from
203 wild-type JE2 using primers:

204 5'- AGAGCTCGAGATGGCTCTATTCAAGAG-3' and 5'-

205 AGATGGATCCTTAAATTGATTTTAAATATTCTTGAC-3' and cloned downstream of the plgT promoter,
206 as described in Potter et al. (2020). The resulting construct was confirmed by whole plasmid

207 sequencing through Plasmidsaurus (Eugene, OR) and will be referred to as pglT here

208 (**Supplementary Figure 1**). The confirmed pglT construct was transformed through electroporation
209 into JE2 *gltT*::Tn, as well as the evolved isolate, EV2. All plasmids were transformed using
210 electroporation (Grosser & Richardson, 2016)

211

212 Analysis of variation of the *S. aureus* *gltT* gene

213 To detect the variation of the *gltT* gene, we assessed a dataset of *S. aureus* genomes that combined
214 380 assemblies from the Staphopia non-redundant diversity set (Petit III & Read, 2018) and 64 CF
215 isolates (Bernardy et al., 2020) to create a dataset of 444 *S. aureus* genome assemblies. Then, we
216 extracted and calculated the number of mutations in the genes *gltT*, *gltS*, *alsT*, *rpoD*, and *agrC*, using a
217 custom software, LIVID (<https://github.com/VishnuRaghuram94/LIVID>), which performs *in-silico* PCR to
218 extract nucleotide regions of interest from genome assemblies and compares the extracted sequence
219 with a user-specified reference region to report mutations. For *gltT*, *gltS*, *alsT*, and *rpoD*, we used the
220 corresponding gene sequences from the *S. aureus* strain JE2 (NCBI RefSeq accession

221 GCF_002993865.1) as a reference. To account for different *agr* groups requiring a different reference
222 sequence, we used the software tool AgrVATE (Raghuram et al., 2022) to calculate the number of
223 mutations in *agrC*. Both LIVID and AgrVATE use Snippy v4.6 for identifying mutations (Seeman, 2015).
224 LIVID was run with the parameters -x 1000 (minimum product size) -y 2000 (maximum product size) -d
225 5 (maximum allowed primer mismatch bases). AgrVATE was run with default parameters, as described
226 in Raghuram et al. (2022) (**Supplementary Table 1**). Mutations labelled as 'synonymous' were single
227 or multi-nucleotide substitutions that did not affect the amino acid sequence. Mutations labelled as 'AA-
228 sequence altering' were single /multi-nucleotide substitutions in-frame insertions/deletions that cause
229 local changes in the amino acid sequence. Putative 'Loss of function' variants include frameshift
230 mutations, start-codon variants and early stops caused by non-synonymous mutations
231 (**Supplementary Table 1**).

232

233 Phenotypic testing for *P. aeruginosa* tolerance

234 *S. aureus* tolerance to *P. aeruginosa* strain PAO1, was determined by coculturing *S. aureus* and PAO1
235 at high initial densities ($>10^8$ CFUs) at a 1:1 ratio for 24 hours and measuring recovered CFUs by
236 serially diluting resuspended cultures and plating on SIA and PIA medias to select for *S. aureus* and *P.*
237 *aeruginosa*, respectively (Bernardy et al., 2020). Phenotyping assays were carried out in 5 separate
238 experiments with 2 biological replicates per strain.

239

240 Murine acute pneumonia model

241 The impact of *gltT* activity on *S. aureus* colonization was determined in a murine acute pneumonia
242 model. All animal procedures were conducted in accordance with the guidelines of the Emory
243 University Institutional Animal Care and Use Committee (IACUC), under approved protocol number
244 PROTO201700441. 8 to 10-week-old C57BL/6 female mice (Jackson Laboratories, Bar Harbor, ME)

245 were anesthetized with a 0.2 mL mixture of ketamine (6.7 mg/mL) and xylazine (1.3 mg/mL)
246 administered through intraperitoneal injection. All mice were euthanized 24 hours post-infection.
247
248 *S. aureus* strains JE2 and JE2 *gltT*::Tn were grown on SIA for 18 to 24 hours at 37°C and resuspended
249 in phosphate buffered saline (PBS) to an OD₆₀₀ of 8, corresponding to ~2 x 10⁹ CFU/mL. Anesthetized
250 mice were infected with 50 µl (~1 x 10⁸ CFU) of *S. aureus* through intranasal administration (25 µL per
251 nostril). Following euthanasia, whole lung and nasal wash were collected aseptically. The lungs were
252 weighed and homogenized in 1 mL of PBS (Bullet Blender Storm 5). Homogenized lungs and nasal
253 wash were serially diluted and plated on SIA to determine CFUs. For the acute pneumonia murine
254 competition infection, JE2 and JE2 *gltT*::Tn were grown on SIA for 18 to 24 hours at 37°C and
255 suspended in PBS to an-OD₆₀₀ of 14, followed by a 1:2 dilution corresponding to ~4.8 x 10⁹ CFU/mL.
256 Anesthetized mice were infected with 12.5 µl of culture of each *S. aureus* strain (~6 x 10⁷ CFU)
257 administered sequentially and single-strain control mice were infected with either 25 µl of JE2 or JE2
258 *gltT*::Tn (~1 x 10⁸ CFU). Following euthanasia, whole lung and nasal wash were collected and
259 processed following the procedures stated above. Serial dilutions were plated on both SIA and LA
260 supplemented with erythromycin (25 µg/mL) to determine CFU, for both strains and JE2 *gltT*::Tn,
261 respectively. Results were analyzed using one-way analysis of variance (ANOVA) corrected with Šidák
262 in GraphPad Prism 9 (**Figure 4**).

263

264 Competitive fitness assay

265 Fluorescently labeled JE2 and JE2 *gltT*::Tn were grown individually and together in complete CDMG
266 (1.1 mM asp and 1.0 mM glu) (+A/+G) and CDMG with additional asp (2.2 mM asp) and no glu added
267 (++A/0G). Cultures were inoculated at initial densities of OD₆₀₀ 0.01 in flasks with 25 mL of media and
268 incubated at 37°C with continuous shaking for 24 hours. CFUs were determined at inoculation, early
269 growth (4 - 8 hours after inoculation) and endpoint (22 - 24 hours after inoculation). Both versions of

270 each strain (JE2.GFP and JE2.DsRed and JE2 *gltT*::Tn.GFP and JE2 *gltT*::Tn.DsRed) were tested in
271 these conditions in replicate experiments (**Figure 3**).

272

273 Amino acid utilization

274 Amplite™ Fluorimetric L-Aspartate (Aspartic Acid) Assay Kit, and Amplite™ Fluorimetric Glutamic Acid
275 Assay Kit *Red Fluorescence* (AAT Bioquest) were used to measure the concentration of aspartate
276 and glutamate, respectively. Cell-free spent media was collected by filtering resuspended cocultures
277 that were grown for 24 hours on TSA plates (as was done for phenotypic testing for *P. aeruginosa*
278 tolerance) through 0.22 µm syringe filters. Spent media was collected from *S. aureus* monocultures and
279 cocultures, as well as PAO1 monocultures and controls. Control conditions were made by inoculating
280 sterile filters with 10 µl of LB or PBS and incubating for 24 hours. Measurements were taken across 3
281 separate experiments, each with 2 replicates for each culture condition.

282

283 Single cell imaging

284 Batch cultures were grown in TSB media supplemented with chloramphenicol 10 µg/mL to maintain
285 fluorescent plasmids. Overnight cultures were diluted 1:100 into 3 mL fresh TSB media and grown to
286 mid-exponential phase in a test tube at 37°C in a shaking incubator (OD₆₀₀ between 0.5-0.8).
287 Subsequently, cells were washed 3 times with PBS to remove antibiotics and diluted to an OD₆₀₀ of 0.1.
288 Finally, a 1:1:1 coculture was prepared consisting of either JE2.DsRed + JE2 *gltT*::Tn.GFP + PAO1 or
289 JE2.GFP + JE2 *gltT*::Tn.DsRed + PAO1. Agarose media was prepared by adding 1.5% agarose to
290 either fresh or depleted TSB media.

291

292 A 1 mL droplet of agarose media was suspended between two coverslips and dried at room
293 temperature for 30 minutes to create a ~3 mm thick slap, which was then cut into 5x5 mm pads. 1 µL of
294 the coculture was added to the pad and dried until the liquid was absorbed. Afterwards the pad was
295 carefully inverted and placed in a glass-bottomed dish (WillCo Wells). 6 pads were added to the same

296 dish with the following media conditions: fresh TSB, depleted TSB from a 3-hour culture, and depleted
297 TSB from a 16-hour culture. Each media condition was inoculated with one of the two strain mixtures. A
298 small piece of water-soaked tissue was added to preserve humidity and the dish was sealed with
299 parafilm. The experiment was repeated four times using different biological replicates on two separate
300 days. We conducted 4 replicate experiments with each labeled version (GFP or DsRed) of each strain
301 being tested twice. Imaging of the samples began 1 hour after the agar pads were inoculated.

302

303 The pads were imaged using a Nikon Ti2 inverted microscope with perfect focus system, equipped with
304 a Hamamatsu ORCA-Flash4.0 V3 Digital CMOS camera, a Nikon NA1.42 60X Plan Apochromat phase
305 contrast oil objective, a SPECTRA-X LED fluorescent light source, and Chroma filter sets. Images were
306 taken every 3 minutes in the phase, GFP, and RFP channels. Cells were kept at 37°C while imaging
307 using a climate-controlled incubator (Oko-lab).

308

309 Image analysis

310 To analyze colony growth, we segmented and tracked colonies using a custom-build pipeline (code is
311 available at: https://github.com/simonvanvliet/PA-SA_Agapads). The time-lapse movies were manually
312 trimmed to remove later time points where cells overlapped in 3D or where excessive cell movement of
313 *P. aeruginosa* was observed. Subsequently, images were registered using the phase_cross_correlation
314 method of scikit-image (van der Walt et al., 2014). Segmentation of colony outlines was done using the
315 Ilastik supervised pixel classification workflow (Berg et al., 2019). Pixels in the multi-channel image
316 (phase, GFP, RFP) were classified in four classes (GFP / DsRed labeled *S. aureus*, *P. aeruginosa*, and
317 background). The classification probabilities were post-processed using custom written python code to
318 extract individual masks for each colony. In short, the probabilities were smoothed with a gaussian
319 kernel and thresholded using a fixed threshold value of 0.5. The masks were then post-processed using

320 a binary closing operation to fill-in gaps between neighboring cells. Finally, small objects were removed,
321 and holes closed.

322

323 Colonies were tracked using a custom written tracking algorithm that matched colonies across
324 subsequent frames based on the minimal center-to-center distance. Tracks were stopped when
325 colonies merged. An automated filtering procedure was used to trim tracks whenever an unexpectedly
326 large change in colony area was observed (indicative of missed colony merger and/or segmentation
327 error).

328

329 Colony growth rate r was calculated as: $r = \frac{1}{\Delta t} \log \frac{A(T)}{A(0)}$, where $A(0)$ and $A(T)$ are the area (in pixels
330 squared) of the colony at the start of the movie and after $T=1$ hour, and where $\Delta t=3$ minutes is the
331 imaging interval. To quantify the spatial arrangement, we calculated the minimal distance reached
332 between the edge of the focal *S. aureus* colony to the closest pixel occupied by *P. aeruginosa*.
333 Colonies within 300 pixels of the image frame were excluded from the analysis, as we could not
334 accurately quantify their spatial arrangement.

335

336 **Results**

337 *gltT* truncation in *S. aureus* is an adaptation to *P. aeruginosa* tolerance

338 Serial transfer experimental evolution generated multiple populations of *S. aureus* with improved
339 survival in the presence of *Pseudomonas aeruginosa* strain PAO1 (referred to as PAO1). At the
340 completion of 8 serial transfers, two out of four experimental populations had significantly increased
341 their relative survival compared to the JE2 ancestral strain. EE1 and EE3 both increased in the number
342 of recovered CFUs by more than 3 orders of magnitude, with about 10^5 CFUs being initially recovered
343 to about 10^8 CFUs recovered after 8 serial transfers (**Figure 1B**). Similar results were observed in

344 replicate experiments. Single individual colonies from evolved *P. aeruginosa*-tolerant populations
345 maintained this phenotype when cultured at a 1:1 ratio with PAO1 for 24 hours (**Supplementary Figure**
346 **2a**).

347

348 We sequenced the genomes of two single colonies from an evolved tolerant population EE1 and
349 compared those sequences to those of colonies from an evolved but still sensitive population EE4 and
350 colonies from control populations which were transferred in parallel with experimental populations but
351 never cocultured with PAO1. Each isolate was screened for its survivability in coculture with PAO1
352 before being sequenced and the pattern of tolerance observed during the evolution experiment was
353 confirmed. In the two colonies sequenced from population EE1, only one mutation site was unique to
354 them, not appearing in any other compared sequence. Each evolved tolerant isolate (EV2 and EV3)
355 had an independent putative loss of function mutation in the gene encoding for the *S. aureus* amino
356 acid transporter, *gltT*. GltT has been previously described as being the sole aspartate transporter in *S.*
357 *aureus* that also interacts with glutamate (Potter et al., 2020; Zeden et al., 2020; Zhao et al., 2018). In
358 isolate EV3, a single nucleotide base substitution G → A introduced an early stop; in isolate EV2, a 4-
359 base-pair deletion resulted in a frameshift mutation (**Figure 2A**). Both mutations occur between 800-
360 1200bp downstream of the start codon and were predicted to truncate the protein by disrupting the 3'
361 portion of the coding region. Both single colony isolates displayed a *P. aeruginosa*-tolerant phenotype
362 compared to their common ancestor, JE2 (**Supplementary Figure 2b**).

363

364 To confirm the linkage between *gltT* disruption and *P. aeruginosa*-tolerant phenotype, we retrieved the
365 *gltT* mariner transposon knockout mutant, SAUSA300_2329 from the Nebraska Transposon Mutant
366 Library (NTML) (Fey et al., 2013). After transducing the mutation to the ancestral JE2 background, we
367 validated the strain by PCR and confirmed that this strain, which we now refer to as JE2 *gltT*::Tn, had
368 improved CFU recovery after coculture with PAO1 compared to its parent (**Figure 2B**). These results

369 confirmed that the *gltT* disruption was responsible for the enhanced fitness of *S. aureus* in coculture
370 with PAO1. When the mutant *gltT* strains were complemented in *trans*, the PAO1 sensitivity phenotype
371 was restored for both the JE2 *gltT*::Tn and evolved isolate EV2 (**Figure 2B**).

372

373 JE2 *gltT*::Tn outcompetes wild-type *S. aureus* in CDMG without glutamate

374 Growing strains individually in CDMG (**Supplementary Table 2**) or rich LB (**Supplementary Figure 3**)
375 media yielded no insights into fitness differences associated with *gltT* disruption. However, we
376 hypothesized that *gltT* mutants may be able to outcompete wild-type *S. aureus* under certain
377 conditions. To test this, we conducted competition experiments with mutant and wild type strains
378 fluorescently labeled with either GFP or DsRed multicopy plasmids. Labeled strains were inoculated in
379 complete CDMG with 1.1 mM asp and 1.0 mM glu (+A/+G) and CDMG with double the amount of
380 aspartate (2.2 mM asp) and no glutamate added (++A/0G). CFU counts from three replicate
381 experiments showed that JE2 and JE2 *gltT*::Tn were equally fit when grown in complete CDMG, with
382 each strain making up about half of the total culture density. Total CFUs were greater than 10⁸ CFUs
383 across all conditions and replicates. However, in the (++A/0G) condition, JE2 *gltT*::Tn outcompeted
384 wild-type JE2 which only made up about 5% of all CFUs recovered from this growth condition (**Figure**
385 **3**).

386

387 Growth rate differences, as measured by single cell microscopy, are not responsible for the *P.*
388 *aeruginosa*-tolerant phenotype

389 Based on results from CDMG assays, we hypothesized that glutamate depletion by PAO1 would
390 reduce the growth rate in nearby JE2 cells, but not in JE2 *gltT*::Tn cells. To test this hypothesis, we
391 conducted single cell microscopy with wild-type JE2 and JE2 *gltT*::Tn and measured fitness by CFU
392 counts after a 24 hour coculture with PAO1 . We conducted single cell image analysis on cocultures
393 with equal starting ratios of JE2, JE2 *gltT*::Tn and PAO1 using agar pads and GFP and DsRed

394 fluorescently labeled strains. We hypothesized that growth rate differences may only be apparent in
395 depleted media conditions as CFU differences were most obvious between JE2 and JE2 *gltT*::Tn when
396 cocultures are inoculated at high initial densities. However, even in depleted TSB collected from a 16
397 hour culture of PAO1, JE2 *gltT*::Tn did not have an observable difference in growth rate compared to
398 wild-type JE2 (**Figure 4**). Moreover, we did not find a dependence of *S. aureus* growth rates for either
399 wild-type JE2 or JE2 *gltT*::Tn based on their proximity to PAO1 colonies (**Supplementary Figure 4**). In
400 fact, the only growth difference observed was a slight advantage for wild-type JE2 in depleted TSB
401 collected from a 3-hour culture of PAO1. Both strains had very low growth rates in the most depleted
402 media condition, TSB collected from a 16-hour culture of PAO1. Morphology of microcolonies were
403 indistinguishable between *S. aureus* strains and no evidence of small colony variants were observed.
404 These results suggest that the growth advantage of JE2 *gltT*::Tn is a population-level trait that is not
405 explained by growth rate differences between it and its isogenic wild-type counterpart.

406

407 *gltT* disruption alters amino acid uptake in *S. aureus* strains

408 We measured concentrations of aspartate and glutamate in cell-free spent media that was collected
409 from 24-hour TSA cultures (monocultures and cocultures with PAO1) of the following *S. aureus* strains:
410 JE2, JE2 *gltT*::Tn, EV2 and complemented strains JE2 *gltT*::Tn (p*gltT*) and EV2 (p*gltT*). These data
411 revealed that aspartate concentration remained highest in all culture conditions where PAO1 was not
412 present (**Figure 5**). In the case of glutamate, there was very little of the amino acid remaining in any
413 culture condition with wild-type or *gltT* complemented *S. aureus* strains even when PAO1 was not
414 present. Both amino acids were present at higher concentrations in the spent media of *S. aureus*
415 monocultures compared that of cocultures or PAO1 monocultures. This suggested that PAO1 was
416 more efficient at metabolizing both aspartate and glutamate than *S. aureus*. Additionally, the levels of
417 remaining glutamate were higher in *S. aureus* cultures of the *gltT* mutant, suggesting that a functional
418 *gltT* locus was essential to utilizing most of the available glutamate (**Figure 5**).

419

420 *gltT* disruption does not impact *S. aureus* host colonization

421 To gain an understanding of the impact of *gltT* disruption in a host environment, we carried out
422 experiments using an acute murine pneumonia model system where mice were infected with JE2
423 *gltT*::Tn, wild type JE2, or both strains in a coinfection. There were similar population sizes of the
424 ancestral JE2 strain and JE2 *gltT*::Tn recovered from both the nasal wash and lung tissue for both
425 single strain cultures and cocultures of the two strains (**Figure 6**). Therefore, we concluded that *gltT*
426 disruption did not greatly impact *S. aureus*' ability to colonize host respiratory tissues.

427

428 *gltT* disruption was rare in diverse *S. aureus* genomes

429 Findings from the evolution experiment and *gltT* mutant phenotyping tests indicated that *gltT* could be
430 disrupted without severe impacts on strain fitness. We therefore, sought to estimate the variability of
431 *gltT* across diverse *S. aureus* lineages, including CF-associated isolates. Previous work had shown that
432 *gltT* is a core gene (Petit III & Read, 2018) and so we were able to look at *gltT* variability by screening a
433 diverse dataset of 444 *S. aureus* genomes representing 380 MLST sequence types. We did not find
434 mutations identical to the ones we saw during our experimental evolution. Furthermore, we identified
435 only one mutation that caused an early stop, at position 1255, truncating the protein by 8 amino acids.
436 This was the only putative non-functional mutant we observed in *gltT* and it was present in only one
437 sample. This putative loss of function mutant was not isolated from a CF-associated infection.

438

439 We did not observe a significant enrichment of mutations in *gltT* when compared to other amino acid
440 transporters in our dataset. We observed 115 occurrences of non-synonymous mutations in *gltT*, with
441 26 distinct mutations, 25 of which were found in < 10 strains. One mutation - a glutamate → aspartate
442 change at position 891, was found in in 71 strains. Overall, these results suggested that *gltT* disruption

443 was rare in *S. aureus*, even compared to other core genes encoding amino acid transporters
444 (**Supplementary Table 1**). This was also true for CF associated isolates which, in our screen, did not
445 have elevated rates of mutation in *gltT* compared to non-CF isolates.

446

447 **Discussion**

448 Impact of inactivation of *S. aureus gltT* gene in *S. aureus-P. aeruginosa* interactions

449 Interactions between *S. aureus* and *P. aeruginosa* have proven to be complex, and dependent on
450 environment and strain background (Bernardy et al., 2020, 2022). Studies have implicated factors such
451 as the *P. aeruginosa* mucoidy phenotype, *Pseudomonas* excreted compounds or toxins, and *S. aureus*
452 metabolic pathways such as the production of acetoin, as important factors in the interspecific
453 interactions between *S. aureus* and *P. aeruginosa* (Barraza & Whiteley, 2021; Bernardy et al., 2020,
454 2022; Camus et al., 2020; Lasse et al., 2022; Zarrella & Khare, 2021). Surprisingly, despite the wealth
455 of research on the coexistence and competition of these species, in our experimental system, we
456 observed mutation of a highly conserved gene, *gltT*, that had not previously been linked to *S. aureus-P.*
457 *aeruginosa* co-occurrence. Our findings indicated that *S. aureus* JE2 and *P. aeruginosa* PAO1 directly
458 compete over limiting glutamate, particularly when grown at high densities on TSA plates. Our evolved
459 isolates appear to have gained a phenotypic advantage over their JE2 ancestor by disrupting the *gltT*
460 locus – limiting import of aspartate and glutamate and likely relying on alternative metabolic pathways.
461 Under the conditions of the evolution experiment we designed here, there is apparently significant
462 selective pressure for *S. aureus* to optimize its amino acid metabolism for a glutamate-limited
463 environment. The *S. aureus gltT* gene was also found to be disrupted in osteomyelitis studies that
464 revealed how excess glutamate competitively inhibits aspartate transport through *gltT* (Potter et al.,
465 2020). While the osteomyelitis study of Potter et al. (2020) presents the inverse of the nutrient
466 landscape *S. aureus* is adapting to in our experiment – a challenge of excess glutamate rather than it
467 being a limiting nutrient - it also demonstrates the importance of exogenous amino acids in *S. aureus*

468 competitive fitness and the importance of altering metabolic pathways as an adaptive strategy in
469 changing environments. Our findings suggest that we still do not understand enough about the
470 interaction between *S. aureus* and *P. aeruginosa* to predict the genes that give adaptive advantages in
471 any given combination of strains and environmental conditions.

472

473 We acknowledge some limitations of our experimental evolution approach. For instance, while fresh
474 PAO1 was introduced to each coculture period we found that a minority population of *P. aeruginosa*
475 were able to survive on SIA agar even though they did not form colonies. We suspect that some *P.*
476 *aeruginosa* cells may have been transferred between coculture periods and could have coevolved with
477 the JE2 populations. However, fresh PAO1 was introduced at each coculture period, and the evolved
478 *P. aeruginosa*-tolerant phenotypes of *S. aureus* were maintained after populations were fully isolated
479 from any retained PAO1. Therefore, any effect of carryover *P. aeruginosa* appeared to have little effect
480 compared to the larger population of fresh introduced ancestral PAO1. Additionally, while the
481 population sizes in our evolution experiment are likely much denser than what occurs during a CF lung
482 infection, populations of *S. aureus* and *P. aeruginosa* have both been observed at levels as high as 10^8
483 CFUs/mL in CF sputum samples collected from coinfecting patients (Fischer et al., 2020)

484

485

486 The role of aspartate and glutamate in *P. aeruginosa* tolerance

487 Previous analysis of *S. aureus* metabolism has shown that glutamate derivatives are required for *S.*
488 *aureus* to metabolize aspartate into oxaloacetate, a secondary metabolite required in the citric acid
489 cycle (Halsey et al., 2017). Therefore, the absence of extracellular glutamate may lead to reduced
490 activity of the TCA cycle. This could explain why all tested *S. aureus* strains showed a reduced growth-
491 rate when glutamate was not present in CDMG compared to complete CDMG (**Supplementary Table**
492 **2**). However, we did not observe significant growth rate differences between wild type JE2 *S. aureus*

493 and JE2 *gltT*::Tn in our CDMG monoculture assays or by single-cell microscopy. These data suggest
494 that despite its important role in amino acid metabolism there were few apparent fitness trade-offs
495 associated with disrupting *gltT* when *P. aeruginosa* is not present in standard laboratory conditions
496 (Zhao et al., 2018). In addition, the finding that *gltT* mutations are extremely rare in non-laboratory
497 adapted stains reinforces the key metabolic role of this core gene. We postulate that continuing to
498 import aspartate in the wild-type strain in the absence of glutamate may lead to a buildup of aspartate
499 intracellularly and a corresponding reduced competitive fitness. This hypothesis is supported by our
500 finding that along with its increased *P. aeruginosa*-tolerance, JE2 *gltT*::Tn was able to outcompete
501 wildtype JE2 in the CDMG condition where additional aspartate was added and no glutamate was
502 added (++A/0G) (**Figure 3**).

503 Further experimentation is needed to better understand how amino acid metabolism facilitates *S.*
504 *aureus*-*P. aeruginosa* interactions; however, we conclude here that in our evolution experiment, *S.*
505 *aureus* is primarily adapting to the limitation of glutamate in its environment by disrupting its aspartate
506 transporter and relying on alternative metabolic pathways to carry out the TCA cycle. In short, the major
507 source of negative selective pressure that *S. aureus* experienced when grown in the presence of *P.*
508 *aeruginosa* was competition over exogenous amino acids.

509

510 Experimental evolution as a useful tool for studying pathogens

511 Experimental or directed evolution experiments carried out in laboratory conditions can be a powerful
512 way to reduce complex adaptive phenotypes in important pathogens like *S. aureus* and *P. aeruginosa*
513 to single genetic determinants. The lab environments used for experimental evolution studies are
514 removed from the conditions we study, such as the cystic fibrosis lung environment or the host
515 environment in general. Despite this however, there is still a lot to be gained from evolution experiments
516 conducted in laboratory conditions with lab-adapted strains. Even if such experiments identify genes
517 that are highly conserved (and thus unlikely to be important for adaptation in the setting of human

518 infection) as we have found in this study, these findings reveal potential adaptive trajectories that may
519 lead to possible treatment targets as well as a greater understanding of pathogen biology and
520 physiology. For instance, our findings here lay important groundwork in the development of coinfection
521 disruption therapy by highlighting the importance of the nutrient landscape in the facilitation of *S.*
522 *aureus*-*P. aeruginosa* coexistence in the cystic fibrosis lung or other chronic infections. The link
523 between *gltT* and *P. aeruginosa* tolerance likely could not have been identified by screening clinical
524 isolates because the gene is so highly conserved. Our *in vitro* experiments suggest that *gltT* mutants
525 can colonize lung tissue just as well as wild-type strains and would be more likely to coexist with
526 *Pseudomonas* in a coinfection. Therefore, even though likely rare, this genotype could be important to
527 screen for when treating coinfections and is certainly important to consider in the development of new
528 therapies to treat polymicrobial infections.

529

530 Acknowledgements

531 This work was supported in part with grants for the National Institutes of Health (R21 AI148847) and the
532 US Cystic Fibrosis Foundation (GOLDBE19I0) to JBG. Research reported in this publication was
533 supported in part by National Institute of Allergy and Infectious Diseases of the National Institutes of
534 Health (T32AI138952), and Emory University and the Infectious Disease Across Scales Training
535 Program (IDASTP) (AMA). The content is solely the responsibility of the authors and does not
536 necessarily represent the official views of the National Institutes of Health, Emory University or IDASTP.

537

538 GB and SVV were supported by an Ambizione grant from the Swiss National Science Foundation (grant
539 no. PZ00P3_202186) and by the University of Basel.

540

541 We would like to thank Rachel Done for her assistance with cloning and strain preparation. We would
542 also like to thank members of the Goldberg and Read labs for their support and review of the
543 manuscript.

544

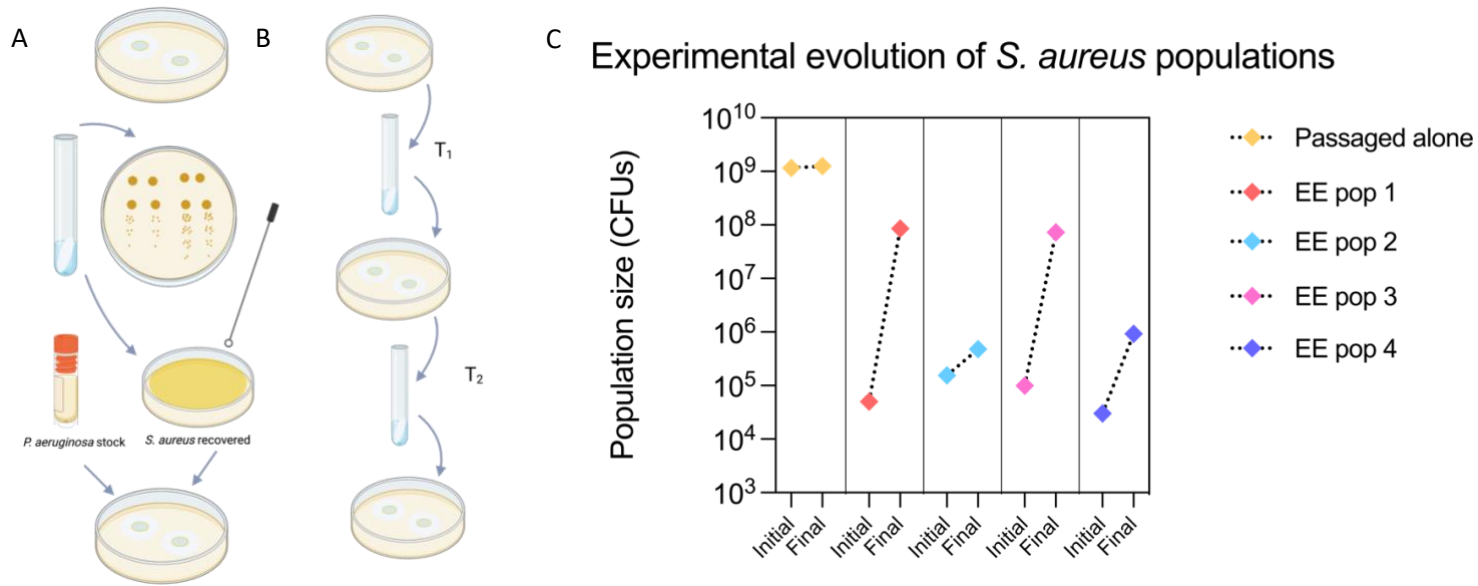
545 **Figures and Tables**

Strain	Description	Plasmid	<i>gltT</i> Genotype	Reference
JE2	USA 300, background for NTML	None	wild type <i>gltT</i>	Fey et. al 2013
PAO1	<i>P. aeruginosa</i> strain			
EV2	Evolved JE2, <i>P. aeruginosa</i> tolerant isolate from EE1	None	1150 4bp deletion	This study
EV3	Evolved JE2, <i>P. aeruginosa</i> tolerant isolate from EE1	None	951 G -> A early stop	This study
JE2 <i>gltT</i>::Tn	NTML transposon mutant NE566 transduced into JE2 background	None	<i>gltT</i> ::Tn	Fey et. al 2013
JE2 <i>gltT</i>::Tn (pglT)	JE2 <i>gltT</i> transposon mutant complemented with pglT construct	pglT	complemented <i>gltT</i>	This study
EV2 (pglT)	Evolved isolate EV2 complemented with pglT construct	pglT	complemented <i>gltT</i>	This study
JE2.GFP	JE2 fluorescently labeled with GFP	pCM29	wild type <i>gltT</i>	Pang et al., 2010
JE2.DsRed	JE2 fluorescently labeled with RFP	pHC48	wild type <i>gltT</i>	lbberson et al., 2016
JE2 <i>gltT</i>::Tn.GFP	JE2 <i>gltT</i> ::Tn fluorescently labeled with GFP	pCM29	<i>gltT</i> ::Tn	Pang et al., 2010
JE2 <i>gltT</i>::Tn.DsRed	JE2 <i>gltT</i> ::Tn fluorescently labeled with RFP	pHC48	<i>gltT</i> ::Tn	lbberson et al., 2016

546

547 **Table 1. List of *Staphylococcus aureus* strains used in this study.** Plasmid pglT was made as part
 548 of this study from the pOS1.plgT vector using methods described in Potter et al. (2020).

549



550

551 **Figure 1. Experimental evolution with *Staphylococcus aureus* USA300 JE2 generates populations**
 552 **that are tolerant to *Pseudomonas aeruginosa* in coculture.** *S. aureus* and *P. aeruginosa* were
 553 cocultured for 48 hours at an inoculation ratio of 30:1 (*S. aureus*:*P. aeruginosa*). A) Transfer procedure -
 554 cocultures are inoculated on solid TSA agar with 0.45 μ m filter paper used to contain and recover the
 555 culture. After the coculture period, filters are resuspended in liquid media and serial dilutions of the
 556 resuspension are spot plated on selective agar. After 24 hours of growth, CFUs are counted for both
 557 species on their respective selective agar SIA and PIA. B) Serial transfer method - a new transfer occurs
 558 when *S. aureus* is isolated from the resuspension by plating 50 μ l on SIA. After overnight incubation, *S.*
 559 *aureus* was inoculated with *P. aeruginosa* from a fresh overnight culture that was diluted to the same
 560 OD₆₀₀. Control populations are repeatedly transferred under the same conditions but never exposed to
 561 *P. aeruginosa*. C) Experimental evolution results: four populations (pop 1-4) were evolved in the presence
 562 of PAO1 for 8 coculture periods; control population (passage alone) never exposed to *P. aeruginosa* also
 563 shown. CFU counts from the first coculture period (initial) and 8th coculture period (final) are shown.

564

565

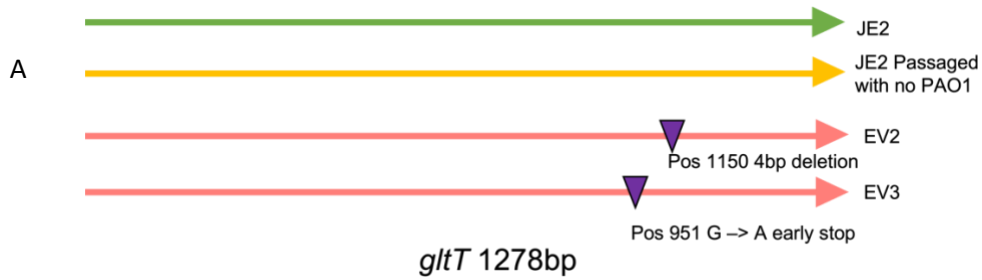
566

567

568

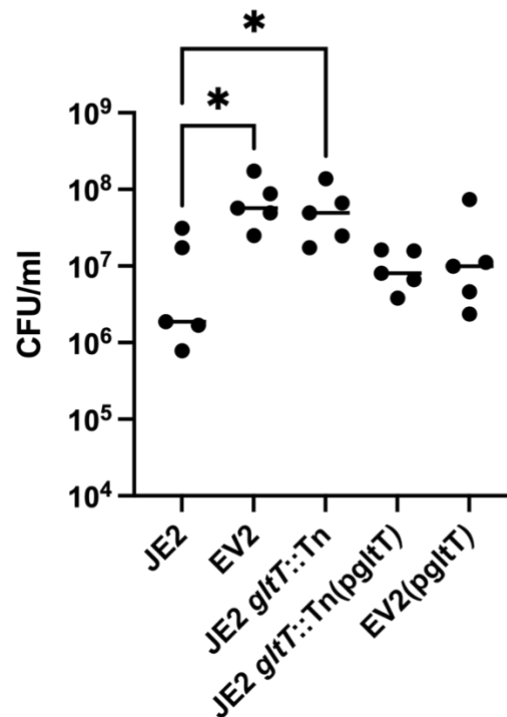
569

570



B

S. aureus recovery after coculture with PAO1

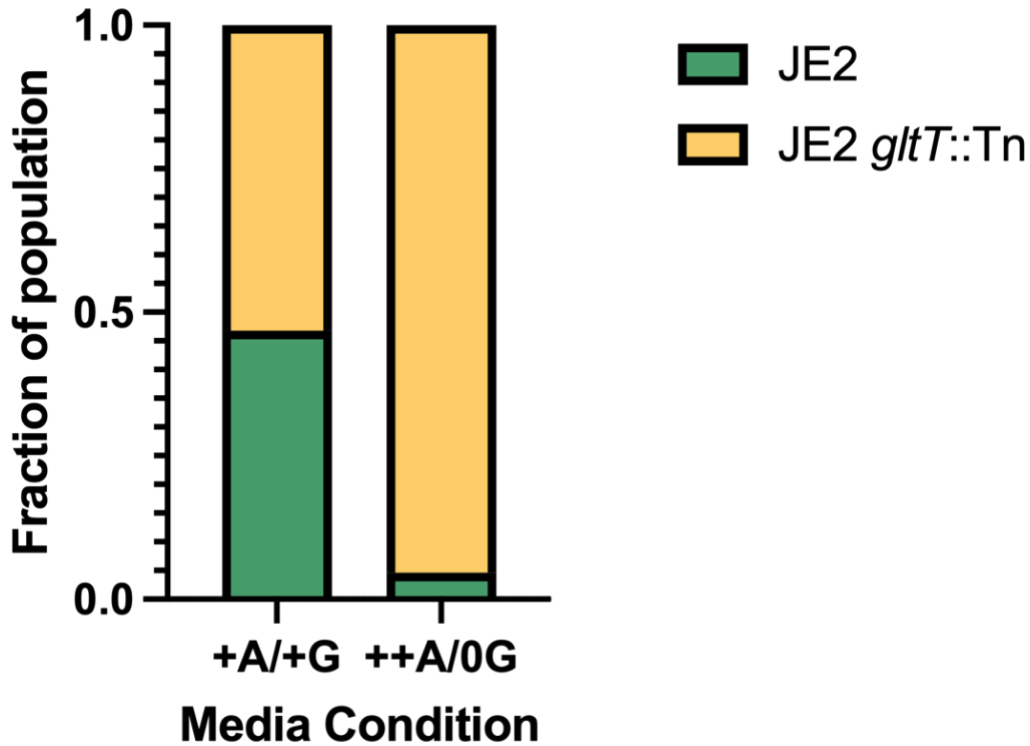


571

572 **Figure 2. *gltT* truncation enhances *S. aureus* recovery after coculture with PAO1.** A) Whole genome
573 sequencing reveals two independent truncations of the aspartate transporter, *gltT*, in sequences of two
574 single colony isolates EV2 and EV3 taken from the same evolved *P. aeruginosa*-tolerant population - EE
575 pop 1 (Fig 1C). B) Evolved phenotype of *P. aeruginosa* tolerance is observed in the *gltT* transposon
576 mutant JE2 *gltT*::Tn and evolved isolate EV2. Wild-type *P. aeruginosa* sensitivity is restored in the
577 complemented transposon mutant JE2 *gltT*::Tn(p*gltT*) and complemented evolved isolate EV2(p*gltT*).
578 Friedman's test for multiple comparisons yielded p-values of 0.0127 and 0.0205 (*) when comparing JE2
579 CFUs to EV2 and JE2 *gltT*::Tn, respectively.

580

581

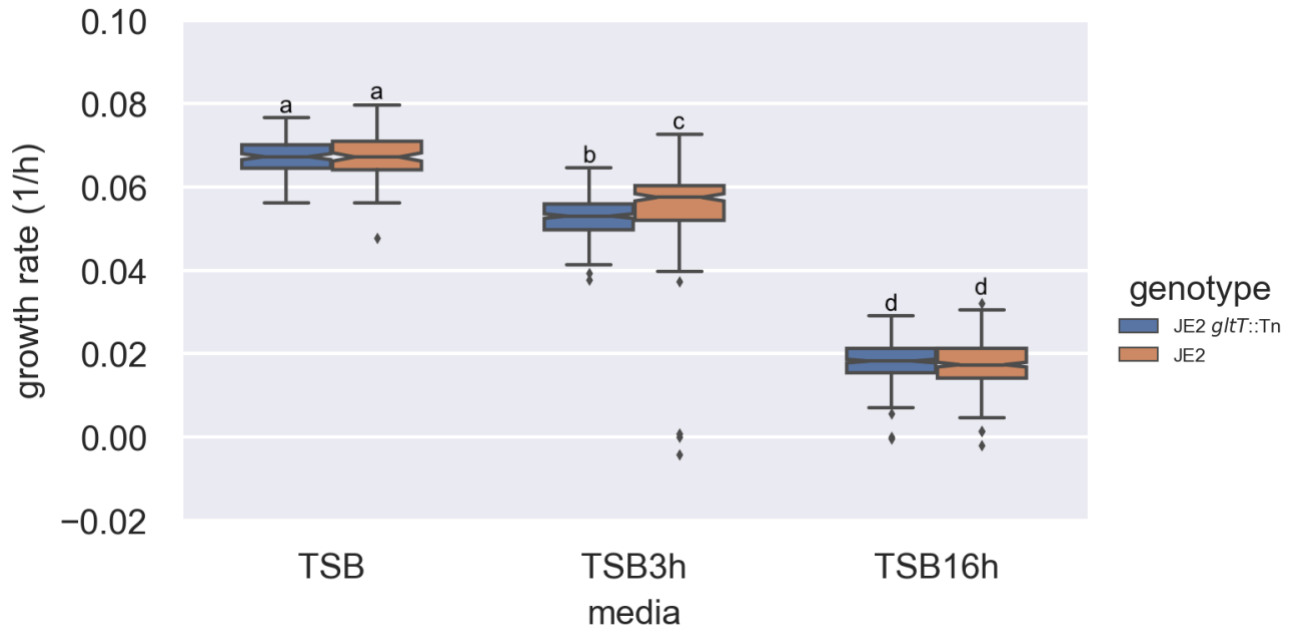


582

583 **Figure 3. JE2 *gltT::Tn* outcompetes wild-type JE2 in CDMG when glutamate is limiting and**
584 **aspartate is in excess.** JE2.GFP, JE2.DsRed and JE2 *gltT::Tn*.GFP and JE2 *gltT::Tn*.DsRed strains
585 labeled with fluorescent plasmids were used to test for competitive fitness in CDMG conditions. One GFP
586 labeled strain and one ds.Red labeled strain were cultured for 24 hours in CDMG media alone and in
587 coculture. Incubated cultures were then serially diluted and incubated overnight at 37°C before CFUs
588 were counted and number of red and green colonies recorded. Each version of each strain was tested at
589 least once across 3 biological replicates. JE2 *gltT::Tn* made up the majority of CFUs recovered after 24
590 hours when aspartate (A) was in excess (++), and glutamate (G) was limited (0G) (++A/0G) Chi-square
591 p-value < 0.0001.

592

593



594

595

596

597

598

599

600

601

602

603

604

605

606

607

608

609

610

611

612

613

614

615

Figure 4. Growth rates of wild-type JE2 and JE2 *gltT::Tn* in coculture with PAO1 in rich and depleted media. Fluorescently labeled strains - JE2.GFP or JE2.DsRed and JE2 *gltT::Tn*.GFP or JE2 *gltT::Tn*.DsRed were cultured together with PAO1 on agar pads made from rich Trypticase Soy Broth (TSB) and depleted cell-free TSB collected from 3 hour and 16-hour PAO1 monocultures. Growth rates of micro colonies were measured using single cell microscopy image analysis. Wild-type JE2 is observed to have a slight growth advantage over mutant JE2 *gltT::Tn* in slightly depleted TSB from a 3-hour culture, however strains grow generally at the same rate in all other conditions. Data was collected over four replicates for each of the two strain combinations. We did not observe consistent differences between the different DsRed or GFP strain combinations and their data was thus pooled. PAO1 also carried a GFP label and was easily distinguished based on cell shape. The two-way ANOVA revealed significant effects of media ($F(2, 18) = 11800.29, p < 0.001$) and genotype ($F(1, 18) = 4.37, p = 0.036$), as well as a significant interaction between media and genotype ($F(2, 18) = 17.55, p < 0.001$) on growth. Post-hoc Tukey's HSD test indicated significant differences between different media conditions ($p < 0.05$), suggesting that the growth varied significantly depending on the media used. Additionally, significant differences were observed between genotypes in the TSB3h media ($p < 0.05$).

616

617

618

619

620

621

622

623

624

625

626

627

628

629

630

631

632

633

634

635

636

637

638

639

640

641

642

643

644

645

646

647

648

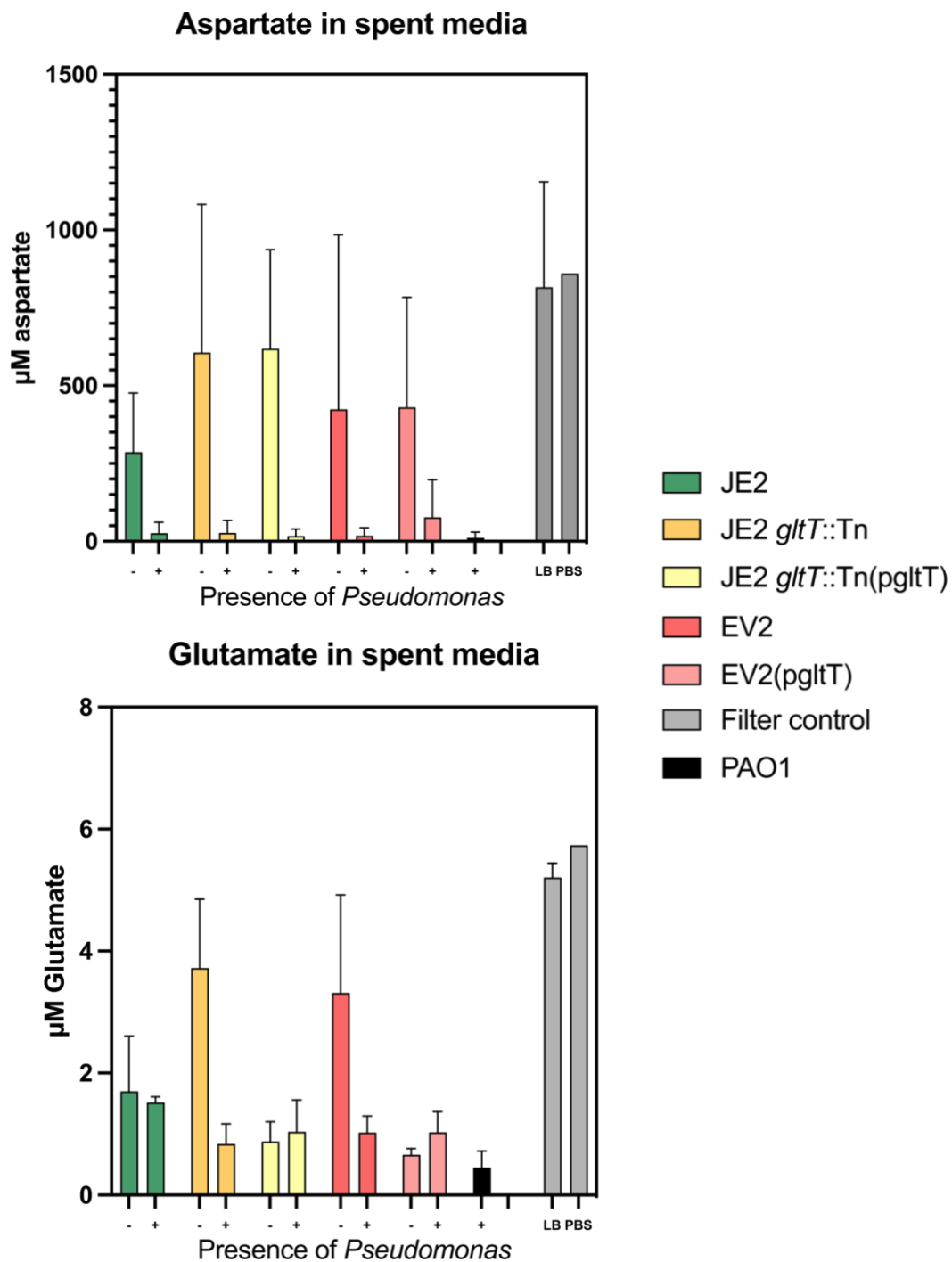
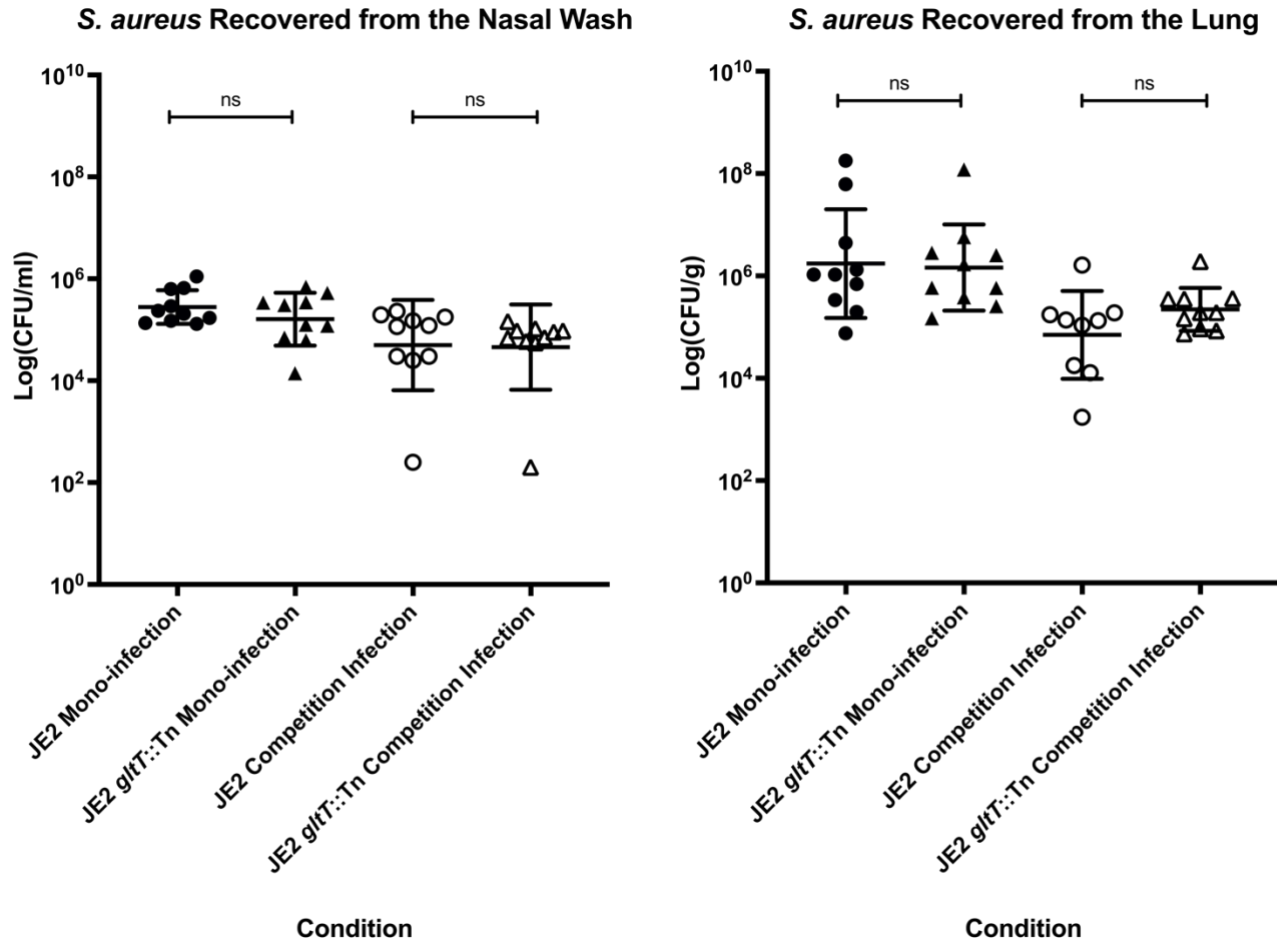


Figure 5. *gltT* is required for *S. aureus* glutamate uptake and aspartate and glutamate are greatly reduced when PAO1 is present. Remaining aspartate and glutamate levels after 24-hours of culturing on 0.45µM filters on TSA plates, were measured using Amplitude Fluorimetric kits. Both cocultures with PAO1 (+) and *S. aureus* monocultures (-) were tested. Control conditions were tested by inoculating filters with 10µL of LB media or 10µL of PBS.



649

650

651 **Figure 6. Colonization ability of *S. aureus* is not impacted by *gltT* genotype.** Similar amounts of *S.*
652 *aureus* are recovered from both lung (left) and nasal wash (right) when JE2 or JE2 *gltT::Tn* are cultured
653 in a mouse alone or in coculture. All mice were euthanized 24 hours post infection. All statistics were
654 performed using GraphPad Prism 9 using one-way analysis of variance (ANOVA) with Šidák correction.
655 Similar levels of colonization in the lungs and upper respiratory tract (nasopharynx) was observed
656 between JE2 and JE2 *gltT::Tn* in 8- to 10-week-old C57BL/6 female mice. For mono-infections, 1×10^8
657 CFU of JE2 and JE2 *gltT::Tn* was administered intranasally. For the competition infections, 6×10^7 CFU
658 of both JE2 and JE2 *gltT::Tn* was sequentially administered intranasally. After 24-hours post-infection,
659 all mice were euthanized and CFUs from the nasal wash and lungs were recovered either on SIA (mono-
660 infection) or both LB + erythromycin (25 μ g/ml) and SIA (competition infection). All statistics were
661 performed using GraphPad Prism 9 using one-way analysis of variance (ANOVA) with Šidák correction.
662

663 REFERENCES

- 664 Barraza, J. P., & Whiteley, M. (2021). A *Pseudomonas aeruginosa* Antimicrobial Affects the
665 Biogeography but Not Fitness of *Staphylococcus aureus* during Coculture. *MBio*, *12*(2), e00047-
666 21. <https://doi.org/10.1128/mBio.00047-21>
- 667 Berg, S., Kutra, D., Kroeger, T., Straehle, C. N., Kausler, B. X., Haubold, C., Schiegg, M., Ales, J.,
668 Beier, T., Rudy, M., Eren, K., Cervantes, J. I., Xu, B., Beuttenmueller, F., Wolny, A., Zhang, C.,
669 Koethe, U., Hamprecht, F. A., & Kreshuk, A. (2019). ilastik: interactive machine learning for
670 (bio)image analysis. *Nature Methods*, *16*(12), 1226–1232. <https://doi.org/10.1038/s41592-019-0582-9>
- 672 Bernardy, E. E., Petit, R. A., Raghuram, V., Alexander, A. M., Read, T. D., & Goldberg, J. B. (2020).
673 Genotypic and Phenotypic Diversity of *Staphylococcus aureus* Isolates from Cystic Fibrosis
674 Patient Lung Infections and Their Interactions with *Pseudomonas aeruginosa*. *MBio*, *11*(3).
675 <https://doi.org/10.1128/mbio.00735-20>
- 676 Bernardy, E. E., Vishnu, R., & Goldberg, J. B. (2022). *Staphylococcus aureus* and *Pseudomonas*
677 *aeruginosa* Isolates from the Same Cystic Fibrosis Respiratory Sample Coexist in Coculture.
678 *Microbiology Spectrum*, *10*(4), e00976-22. <https://doi.org/10.1128/spectrum.00976-22>
- 679 Bolger, A. M., Lohse, M., & Usadel, B. (2014). Trimmomatic: a flexible trimmer for Illumina sequence
680 data. *Bioinformatics (Oxford, England)*, *30*(15), 2114–2120.
681 <https://www.ncbi.nlm.nih.gov/pubmed/24695404>
- 682 Brown, S. P., Cornforth, D. M., & Mideo, N. (2012). Evolution of virulence in opportunistic pathogens:
683 generalism, plasticity, and control. *Trends in Microbiology*, *20*(7), 336–342.
684 <https://doi.org/10.1016/j.tim.2012.04.005>
- 685 Brown, S. P., Le Chat, L., & Taddei, F. (2008). Evolution of virulence: triggering host inflammation
686 allows invading pathogens to exclude competitors. *Ecology Letters*, *11*(1), 44–51.
687 <https://doi.org/10.1111/j.1461-0248.2007.01125.x>
- 688 Bubeck Wardenburg, J., Williams, W. A., & Missiakas, D. (2006). Host defenses against
689 *Staphylococcus aureus* infection require recognition of bacterial lipoproteins. *Proceedings of the*
690 *National Academy of Sciences*, *103*(37), 13831–13836. <https://doi.org/10.1073/pnas.0603072103>
- 691 Camus, L., Briaud, P., Bastien, S., Elsen, S., Doléans-Jordheim, A., Vandenesch, F., & Moreau, K.
692 (2020). Trophic cooperation promotes bacterial survival of *Staphylococcus aureus* and
693 *Pseudomonas aeruginosa*. *The ISME Journal*, *14*(12), 3093–3105. <https://doi.org/10.1038/s41396-020-00741-9>
- 695 Chen, J., Yoong, P., Ram, G., Torres, V. J., & Novick, R. P. (2014). Single-copy vectors for integration
696 at the SaPI1 attachment site for *Staphylococcus aureus*. *Plasmid*, *76*, 1–7.
697 <https://doi.org/https://doi.org/10.1016/j.plasmid.2014.08.001>
- 698 Cystic Fibrosis Foundation. (2021). *Cystic Fibrosis Foundation patient registry 2021 annual data report*.
- 699 Dalton, T., Dowd, S. E., Wolcott, R. D., Sun, Y., Watters, C., Griswold, J. A., & Rumbaugh, K. P.
700 (2011). An In Vivo Polymicrobial Biofilm Wound Infection Model to Study Interspecies Interactions.
701 *PLOS ONE*, *6*(11), e27317-. <https://doi.org/10.1371/journal.pone.0027317>

- 702 Fey, P. D., Endres, J. L., Yajjala, V. K., Widhelm, T. J., Boissy, R. J., Bose, J. L., & Bayles, K. W.
703 (2013). A Genetic Resource for Rapid and Comprehensive Phenotype Screening of Nonessential
704 *Staphylococcus aureus* Genes. *MBio*, 4(1), e00537-12-e00537.
705 <https://doi.org/10.1128/mbio.00537-12>
- 706 Filkins, L. M., Graber, J. A., Olson, D. G., Dolben, E. L., Lynd, L. R., Bhujju, S., & O'Toole, G. A. (2015).
707 Coculture of *Staphylococcus aureus* with *Pseudomonas aeruginosa* Drives *S. aureus* towards
708 Fermentative Metabolism and Reduced Viability in a Cystic Fibrosis Model. *Journal of*
709 *Bacteriology*, 197(14), 2252–2264. <https://doi.org/10.1128/jb.00059-15>
- 710 Fischer, A. J., Singh, S. B., LaMarche, M. M., Maakestad, L. J., Kienenberger, Z. E., Peña, T. A., Stoltz,
711 D. A., & Limoli, D. H. (2020). Sustained Coinfections with *Staphylococcus aureus* and
712 *Pseudomonas aeruginosa* in Cystic Fibrosis. *American Journal of Respiratory and Critical Care*
713 *Medicine*, 203(3), 328–338. <https://doi.org/10.1164/rccm.202004-1322OC>
- 714 Grosser, M. R., & Richardson, A. R. (2016). Method for Preparation and Electroporation of *S. aureus*
715 and *S. epidermidis*. In J. L. Bose (Ed.), *The Genetic Manipulation of Staphylococci: Methods and*
716 *Protocols* (pp. 51–57). Springer New York. https://doi.org/10.1007/7651_2014_183
- 717 Halsey, C., Shulei, L., K, W. J., K, L. M., S, N. A., Laurey, S., Marat, S., Robert, P., & D, F. P. (2017).
718 Amino Acid Catabolism in *Staphylococcus aureus* and the Function of Carbon Catabolite
719 Repression. *MBio*, 8(1), e01434-16. <https://doi.org/10.1128/mBio.01434-16>
- 720 Hamelin, F. M., Allen, L. J. S., Bokil, V. A., Gross, L. J., Hilker, F. M., Jeger, M. J., Manore, C. A.,
721 Power, A. G., Rúa, M. A., & Cunniffe, N. J. (2019). Coinfections by noninteracting pathogens are
722 not independent and require new tests of interaction. *PLOS Biology*, 17(12), e3000551-
723 <https://doi.org/10.1371/journal.pbio.3000551>
- 724 Iandolo, J. J., Worrell, V., Groicher, K. H., Qian, Y., Tian, R., Kenton, S., Dorman, A., Ji, H., Lin, S.,
725 Loh, P., Qi, S., Zhu, H., & Roe, B. A. (2002). Comparative analysis of the genomes of the
726 temperate bacteriophages $\phi 11$, $\phi 12$ and $\phi 13$ of *Staphylococcus aureus* 8325. *Gene*, 289(1), 109–
727 118. [https://doi.org/https://doi.org/10.1016/S0378-1119\(02\)00481-X](https://doi.org/https://doi.org/10.1016/S0378-1119(02)00481-X)
- 728 Ibberson, C. B., Parlet, C. P., Kwiecinski, J., Crosby, H. A., Meyerholz, D. K., & Horswill, A. R. (2016).
729 Hyaluronan Modulation Impacts *Staphylococcus aureus* Biofilm Infection. *Infection and Immunity*,
730 84(6), 1917–1929. <https://doi.org/10.1128/IAI.01418-15>
- 731 Kennedy, A. D., Otto, M., Braughton, K. R., Whitney, A. R., Chen, L., Mathema, B., Mediavilla, J. R.,
732 Byrne, K. A., Parkins, L. D., Tenover, F. C., Kreiswirth, B. N., Musser, J. M., & DeLeo, F. R.
733 (2008). Epidemic community-associated methicillin-resistant *Staphylococcus aureus*: Recent
734 clonal expansion and diversification. *Proceedings of the National Academy of Sciences*, 105(4),
735 1327–1332. <https://doi.org/10.1073/pnas.0710217105>
- 736 Kennedy, A. D., Porcella, S. F., Martens, C., Whitney, A. R., Braughton, K. R., Chen, L., Craig, C. T.,
737 Tenover, F. C., Kreiswirth, B. N., Musser, J. M., & DeLeo, F. R. (2010). Complete Nucleotide
738 Sequence Analysis of Plasmids in Strains of *Staphylococcus aureus* Clone USA300 Reveals a
739 High Level of Identity among Isolates with Closely Related Core Genome Sequences. *Journal of*
740 *Clinical Microbiology*, 48(12), 4504–4511. <https://doi.org/10.1128/jcm.01050-10>

- 741 Krausz, K. L., & Bose, J. L. (2016). Bacteriophage Transduction in *Staphylococcus aureus*: Broth-
742 Based Method. In J. L. Bose (Ed.), *The Genetic Manipulation of Staphylococci: Methods and*
743 *Protocols* (pp. 63–68). Springer New York. https://doi.org/10.1007/7651_2014_185
- 744 Lasse, K., Stephanie, C., H, C. M., Rita, L., Morten, A., Maria, A., Dan, S., & Thomas, B. (2022).
745 Investigation of the Mechanism and Chemistry Underlying *Staphylococcus aureus*' Ability to Inhibit
746 *Pseudomonas aeruginosa* Growth In Vitro. *Journal of Bacteriology*, *204*(11), e00174-22.
747 <https://doi.org/10.1128/jb.00174-22>
- 748 Limoli, D. H., Whitfield, G. B., Kitao, T., Ivey, M. L., Davis, M. R., Grahl, N., Hogan, D. A., Rahme, L. G.,
749 Howell, P. L., O'Toole, G. A., & Goldberg, J. B. (2017). *Pseudomonas aeruginosa* Alginate
750 Overproduction Promotes Coexistence with *Staphylococcus aureus* in a Model of Cystic Fibrosis
751 Respiratory Infection. *MBio*, *8*(2), e00186-17. <https://doi.org/10.1128/mBio.00186-17>
- 752 Limoli, D. H., Yang, J., Khansaheb, M. K., Helfman, B., Peng, L., Stecenko, A. A., & Goldberg, J. B.
753 (2016). *Staphylococcus aureus* and *Pseudomonas aeruginosa* co-infection is associated with
754 cystic fibrosis-related diabetes and poor clinical outcomes. *European Journal of Clinical*
755 *Microbiology & Infectious Diseases*, *35*(6), 947–953. <https://doi.org/10.1007/s10096-016-2621-0>
- 756 Mashburn, L. M., Jett, A. M., Akins, D. R., & Whiteley, M. (2005). *Staphylococcus aureus* Serves as an
757 Iron Source for *Pseudomonas aeruginosa* during In Vivo Coculture. *Journal of Bacteriology*,
758 *187*(2), 554–566. <https://doi.org/10.1128/jb.187.2.554-566.2005>
- 759 Nguyen, A. T., O'Neill, M. J., Watts, A. M., Robson, C. L., Lamont, I. L., Angela, W., & Oglesby-
760 Sherrouse, A. G. (2014). Adaptation of Iron Homeostasis Pathways by a *Pseudomonas*
761 *aeruginosa* Pyoverdine Mutant in the Cystic Fibrosis Lung. *Journal of Bacteriology*, *196*(12), 2265–
762 2276. <https://doi.org/10.1128/JB.01491-14>
- 763 Orazi, G., & O'Toole, G. A. (2017). *Pseudomonas aeruginosa* Alters *Staphylococcus aureus* Sensitivity
764 to Vancomycin in a Biofilm Model of Cystic Fibrosis Infection. *MBio*, *8*(4), e00873-17.
765 <https://doi.org/10.1128/mBio.00873-17>
- 766 Pang, Y. Y., Schwartz, J., Thoendel, M., Ackermann, L. W., Horswill, A. R., & Nauseef, W. M. (2010).
767 agr-Dependent Interactions of *Staphylococcus aureus* USA300 with Human Polymorphonuclear
768 Neutrophils. *Journal of Innate Immunity*, *2*(6), 546–559. <https://doi.org/10.1159/000319855>
- 769 Petit III, R. A., & Read, T. D. (2018). *Staphylococcus aureus* viewed from the perspective of 40,000+
770 genomes. *PeerJ*, *6*, e5261. <https://doi.org/10.7717/peerj.5261>
- 771 Potter, A. D., Butrico, C. E., Ford, C. A., Curry, J. M., Trenary, I. A., Tummarakota, S. S., Hendrix, A. S.,
772 Young, J. D., & Cassat, J. E. (2020). Host nutrient milieu drives an essential role for aspartate
773 biosynthesis during invasive *Staphylococcus aureus* infection. *Proceedings of the National*
774 *Academy of Sciences*, *117*(22), 12394–12401. <https://doi.org/10.1073/pnas.1922211117>
- 775 Raghuram, V., M, A. A., Qi, L. H., A, P. R., B, G. J., & D, R. T. (2022). Species-Wide Phylogenomics of
776 the *Staphylococcus aureus* Agr Operon Revealed Convergent Evolution of Frameshift Mutations.
777 *Microbiology Spectrum*, *10*(1), e01334-21. <https://doi.org/10.1128/spectrum.01334-21>
- 778 Schneewind, O., Model, P., & Fischetti, V. A. (1992). Sorting of protein a to the staphylococcal cell wall.
779 *Cell*, *70*(2), 267–281. [https://doi.org/10.1016/0092-8674\(92\)90101-H](https://doi.org/10.1016/0092-8674(92)90101-H)

- 780 Seeman, T. (2015). *snippy: fast bacterial variant calling from NGS reads*.
781 <https://github.com/tseemann/snippy>
- 782 Silberstein, E., Serna, C., Fragoso, S. P., Nagarkatti, R., & Debrabant, A. (2018). A novel
783 nanoluciferase-based system to monitor *Trypanosoma cruzi* infection in mice by bioluminescence
784 imaging. *PLOS ONE*, *13*(4), e0195879-. <https://doi.org/10.1371/journal.pone.0195879>
- 785 Stacy, A., Fleming, D., Lamont, R. J., Rumbaugh, K. P., & Whiteley, M. (2016). A Commensal
786 Bacterium Promotes Virulence of an Opportunistic Pathogen via Cross-Respiration. *MBio*, *7*(3),
787 e00782-16. <https://doi.org/10.1128/mBio.00782-16>
- 788 van der Walt, S., Schönberger, J. L., Nunez-Iglesias, J., Boulogne, F., Warner, J. D., Yager, N.,
789 Gouillart, E., Yu, T., & contributors, the scikit-image. (2014). scikit-image: image processing in
790 Python. *PeerJ*, *2*, e453. <https://doi.org/10.7717/peerj.453>
- 791 Wadsworth, C. B., Arnold, B. J., Abdul, S. M. R., & Grad, Y. H. (2018). Azithromycin Resistance
792 through Interspecific Acquisition of an Epistasis-Dependent Efflux Pump Component and
793 Transcriptional Regulator in *Neisseria gonorrhoeae*. *MBio*, *9*(4), 10.1128/mbio.01419-18.
794 <https://doi.org/10.1128/mbio.01419-18>
- 795 Wieneke, M. K., Felix, D., Claudia, N., Dennis, G., Lena, K., Theo, T., Angelika, D., Christina, K., Jörg,
796 G.-O., Peter, K., Holger, S., Bianca, S., Johannes, R., Jerzy-Roch, N., Janina, T., Julia, P., Marie,
797 B. J., Mariele, S., Miriam, A., ... Kahl, B. C. (2021). Association of Diverse *Staphylococcus aureus*
798 Populations with *Pseudomonas aeruginosa* Coinfection and Inflammation in Cystic Fibrosis Airway
799 Infection. *MSphere*, *6*(3), e00358-21. <https://doi.org/10.1128/mSphere.00358-21>
- 800 Wingett, S. W., & Andrews, S. (2018). FastQ Screen: A tool for multi-genome mapping and quality
801 control [version 2; peer review: 4 approved]. *F1000Research*, *7*(1338).
802 <https://doi.org/10.12688/f1000research.15931.2>
- 803 Zarrella, T. M., & Khare, A. (2021). Systematic identification of molecular mediators underlying sensing
804 of *Staphylococcus aureus* by *Pseudomonas*
805 *aeruginosa*. *BioRxiv*, 2021.10.24.465352. <https://doi.org/10.1101/2021.10.24.465352>
- 806 Zeden, M. S., Kviatkovski, I., Schuster, C. F., Thomas, V. C., Fey, P. D., & Gründling, A. (2020).
807 Identification of the main glutamine and glutamate transporters in *Staphylococcus aureus* and their
808 impact on c-di-AMP production. *Molecular Microbiology*, *113*(6), 1085–1100.
809 <https://doi.org/https://doi.org/10.1111/mmi.14479>
- 810 Zhao, H., Roistacher, D. M., & Helmann, J. D. (2018). Aspartate deficiency limits peptidoglycan
811 synthesis and sensitizes cells to antibiotics targeting cell wall synthesis in *Bacillus subtilis*.
812 *Molecular Microbiology*, *109*(6), 826–844. <https://doi.org/https://doi.org/10.1111/mmi.14078>
- 813